

DC Motor Drive System

Cascade Control Strategy

Mahmoud Abdalla, Mohammad Alsharif, Utkarsha Atkare, Rishikesh Bagwe, Mawla Boaks, Roshen Borkar, Dorian Brown

Department of Electrical and Computer Engineering

Purdue School of Engineering and Technology

IUPUI

Abstract—Engineering applications rely on the use of control techniques to optimize their performance and efficiency. These applications include DC machines (DC motors and generators). The control of DC machines involves several parameters such as current, voltage and speed. The type of controller used depends on multiple factors such as the amount of noise and frequency response required for the machine. The aim of this project is to design a PI controller to control the electrical current and speed of a DC motor. In order to meet the given design requirements, certain analytical tools were utilized such as feedback loop control, stability criteria and tuning techniques. In addition, computer simulations using MATLAB and Simulink were used to test the performance and prove the validity of the analytical results of the design.

Keywords—DC Motor; Cascade Configuration; PI Controller; Simulink; Matlab; Speed Control

I. INTRODUCTION

Using feedback control systems, strategies to manipulate speed can be achieved in DC motors by applying specific parameters to current or voltage controllers. For this instance, speed control is implemented using a cascade configuration. This design scheme uses an outer feedback loop for speed control and an inner loop for armature current. Due to the different dynamics between the loops, with the inner loop being much faster than the outer loop, we observe some control from each controller. We use two PI controllers, $C_o(S)$ and $C_i(S)$, to guarantee null error for DC armature current and speed. Advantages of cascade control include reduced armature current and preventing damage to the machine.

II. DC MOTORS

A. Working Principle

The DC Motor is a type of electrical machine that converts electrical energy to mechanical energy by the magnetic field that is generated by the current travelling through the coil. It is mandatory to have some sort of mechanism to change the direction of current flow in the rotor coils so that a complete rotation can be executed.

The DC motor consists of a stator that provides the constant magnetic field and a simple coil rotor. In most cases the rotor rotates inside the stator. The supply voltage to the rotor is provided by commutator rings in contact with brushes and connected to a power supply. The rotor coil is usually wound on a highly permeable steel layer to encourage flux interaction.

The stator is magnetized by a power supply, in small applications permanent magnets, while the rotor coil is energized. When the rotor coil conducts current an electromagnetic field is generated producing a rotational force according to Lorentz Law. As the commutator ring rotates it connects with the opposite polarity and as a result the current travels in opposite direction resulting in full rotation of the rotor coil. As the rotor coil is perpendicular to the magnetic field there is a drop in torque, compensated by adding another loop in the rotor with separate commutator rings.

The stator can be energized in 2 ways: parallel or series. The Series configuration has a good starting torque but its speed drops drastically with the load whereas the parallel configuration has an almost constant speed however the starting torque is low. One of the major applications of DC motor is the universal motor which can run on both AC and DC supply.

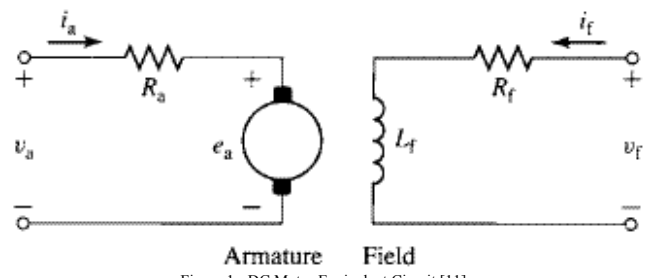


Figure 1 - DC Motor Equivalent Circuit [11]

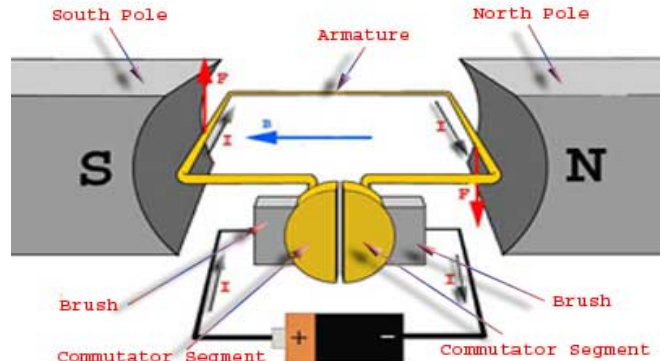
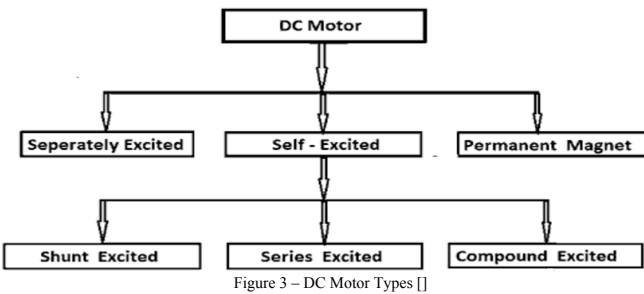


Figure 2 - DC Motor Working Principle [10]

A DC motor can be classified based on various categories like size, output torque range, field winding excitation, etc. Conventionally they are divided based on the type of field winding (electromagnet) excitation whether it's separately excited, self-excited or has permanent magnet for field poles.



B. Types of DC Motors

Based on the type they exhibit different speed and torque characteristics and their speed control methods also vary. The self excited shunt wound DC motor is most widely used in industrial applications. A DC motor is also distinguished as a brushed or brushless DC motor. But only separately excited and self excited DC motors are discussed in this report. The motor used in this project is a separately excited DC motor.

- Separately Excited DC Motor:

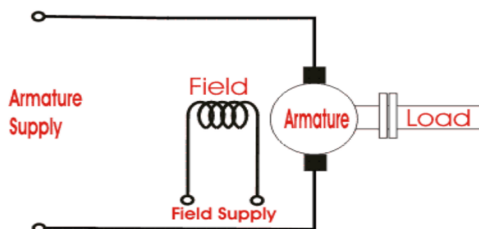


Figure 4 – Separately Excited DC Motor [10]

A separately excited DC motor's field coil is energized from a separate DC voltage source and the armature coil is given another DC voltage. Figure 4 shows a simple wiring diagram of this type of motor. The two coils are isolated to each other and does give more ways for regulation the characteristics of the motor. So the speed control can be achieved by varying the field as well as armature DC voltage independently. These types of DC motor are often used as actuators, in trains and for automatic traction purpose.

- Shunt DC Motor:

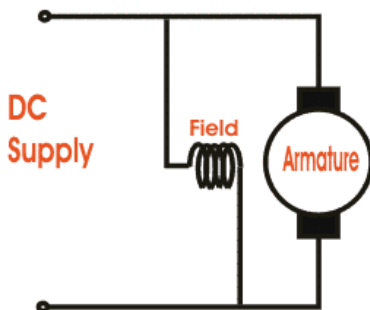


Figure 5 – Shunt DC Motor [10]

A shunt wound DC motor is a self-excited DC motor, where the field windings are connected in parallel to the armature winding of the motor. In this motor, both the armature and field windings absorb the same amount of supply voltage. This motor is known for its constant speed as it does not change with the variation of the mechanical load

on the output. This fact can be explained through the following equations:

$$E = E_b + I_a R_a \quad (1)$$

Where E , E_b , I_a , R_a are the supply voltage, back EMF, armature current and armature resistance respectively.

$$E_b = k_a \varphi \omega \quad (2)$$

Where k_a , φ , ω are the winding constant, field flux and angular speed respectively. Substituting Eq. (2) into Eq. (1) and solving for w

$$\omega = \frac{E - I_a R_a}{k_a \varphi} \quad (3)$$

The torque equation of a DC motor is:

$$T_g = k_a \varphi I_a \quad (4)$$

Therefore, the speed-torque curve can be plotted as below

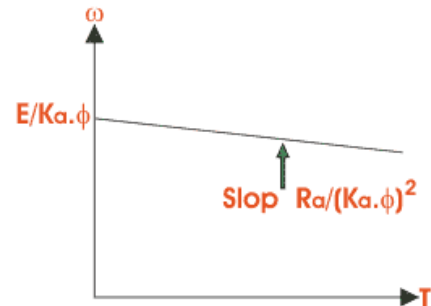


Figure 6 – Speed Versus Torque Curve for shunt DC Motor [10]

- Series DC Motor:

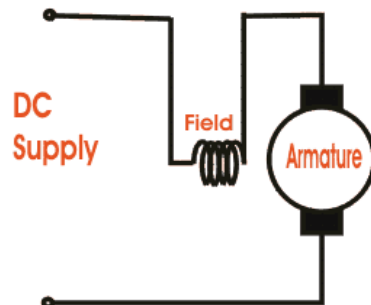


Figure 7 – Series DC Motor Circuit [10]

A series wound DC motor is a self-excited DC motor, where the field winding is connected in series to the armature winding. In this motor, the armature and field windings share the same current. In terms of behavior, the main difference between the shunt and series motor is the fact that in the series motor the speed is not constant but it changes with the variation of the torque load. This behavior can be explained through the following equations:

$$E = E_b + I_a (R_a + R_f) \quad (5)$$

Where R_f is the field resistance

The back EMF remains the same as in Eq. (2) except the flux is now expressed as:

$$\varphi = cI_a = cI_f \quad (6)$$

Where c is a constant of proportionality.

Substituting Eq. (6) into Eq. (2):

$$E_b = k_a c I_a \omega \quad (7)$$

Substituting Eq. (7) into Eq. (5) and solving for ω

$$\omega = \frac{E}{k_a c I_a} - \frac{R_a + R_f}{k_a c} \quad (8)$$

From Eq. (8) and Eq. (4) the speed torque curve can be plotted shown below.

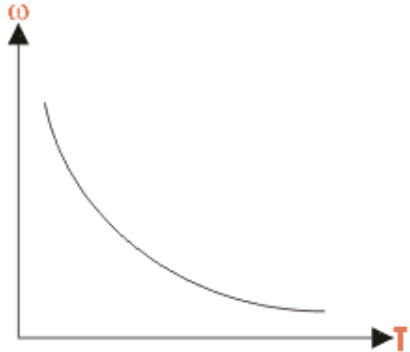


Figure 8 – Speed Versus Torque Curve for a Series DC Motor [10]

- Compound DC Motor:

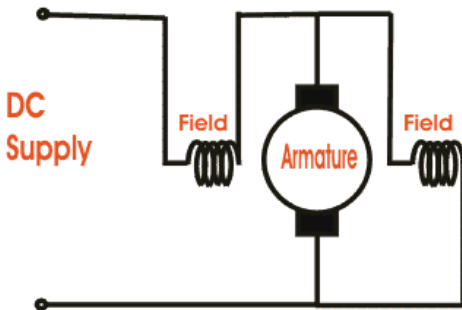


Figure 9 – Compound DC Motor Circuit [10]

A compound wound DC motor is a self-excited DC motor that is a combination of the series and shunt motors. It has a series field winding that is connected in series with the armature and a shunt field that is in parallel with the armature. This configuration allows the motor to have the torque characteristics of the series motor and the speed characteristics of the shunt motor.

There are two types of compound DC motors: cumulative and differential. A compound motor is cumulative when the shunt field flux assists the main field flux, produced by the main field connected in series to the armature winding shown by: $\varphi_{total} = \varphi_{series} + \varphi_{shunt}$

It is differential when the arrangement of the shunt and series winding is such that the field flux produced by the shunt field winding diminishes the effect of flux by the main series field winding show by: $\varphi_{total} = \varphi_{series} - \varphi_{shunt}$

Below shows the speed-torque curve of the cumulative and differential compound DC motors compared to the shunt and series DC motors.

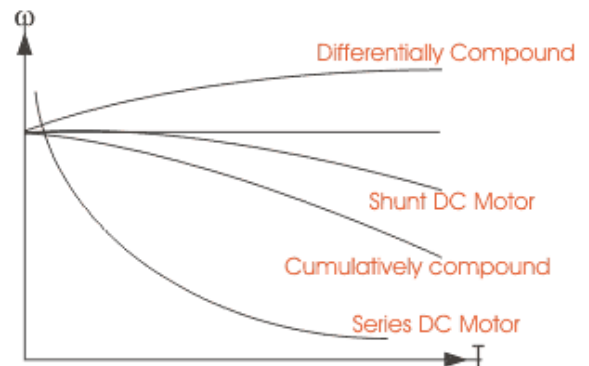


Figure 10 – Speed Versus Torque Curve for Cumulative, Differential, Shunt, and Series DC Motor [10]

C. Dynamic Equations, Block Diagrams, State Equations

In addition to the types of DC motors, understanding how the field and armature circuits interact with each other is critical to further analysis of less practical DC machines. Operation of DC components allows us to first assume the following for simplicity: current flowing through the field winding creates a magnetic field causing revolutions of the armature coils, rotations of the armature coils induces voltage however operation of the commutator eliminates induced voltage in one coil as a result of current change over time in the other coil. When considering voltage and torque equations, it is sufficient to conclude a dynamic set of equations to avoid length derivations shown below.

$$v_a = R_a i_a + L_a \frac{di_a}{dt} + e_a \quad (9)$$

$$v_f = R_f i_f + L_f \frac{di_f}{dt} \quad (10)$$

$$T_e - T_l - B_m w_r = J_m \frac{d\omega_r}{dt} \quad (11)$$

Furthermore, analysis of system control for DC machines uses these dynamic equations for block diagram and state equation representation of a DC control system. Rewriting equations 9, 10, and 11 as functions of derivatives we obtain:

$$\frac{di_a}{dt} = \frac{v_a}{L_a} - \frac{K_c \lambda_f}{L_a} w_r - \frac{R_a}{L_a} i_a \quad (12)$$

$$\frac{di_f}{dt} = \frac{v_f}{L_f} - \frac{R_f}{L_f} i_f \quad (13)$$

$$\frac{d\omega_r}{dt} = \frac{K_c \lambda_f}{J_m} i_a - \frac{T_l}{J_m} - \frac{B_m}{J_m} w_r \quad (14)$$

Taking the Laplace Transform, we can transform equations 12, 13, and 14 into transfer functions. This is the form needed for block diagram representation of DC motor control:

$$\frac{I_a}{V_a - E_a} = \frac{1}{R_a + sL_a} \quad (17)$$

$$\frac{I_f}{V_f} = \frac{1}{R_f + sL_f} \quad (18)$$

$$\frac{W_r}{T_e - T_e} = \frac{1}{B_m + sJ_m} \quad (19)$$

The DC Motor Control Block Diagram is represented below. As illustrated the block diagrams represent the armature, field, and torque control parameters necessary for system control and stability.

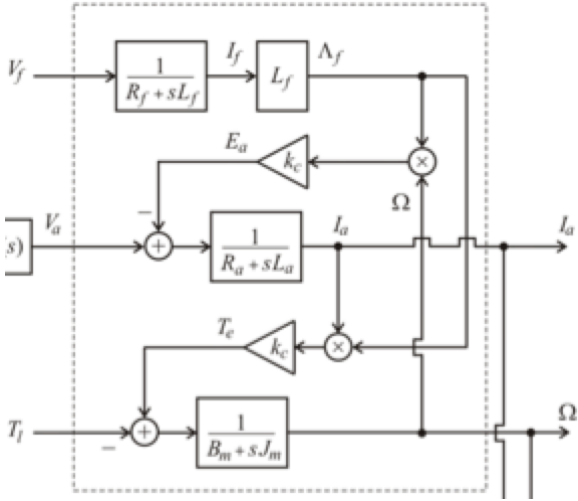


Figure 11 - DC Control Block Diagram [13]

Additionally, state equations can be obtained from the dynamic equations of a DC Motor by representation in matrix form:

$$\frac{d}{dt} \begin{bmatrix} i_a \\ w_r \end{bmatrix} = \begin{bmatrix} -R_a/L_a & K_c \lambda_f / L_a \\ K_c \lambda_f / J_m & -B_m / J_m \end{bmatrix} \begin{bmatrix} i_a \\ w_r \end{bmatrix} + \begin{bmatrix} 1/L_a & 0 \\ 0 & -1/J_m \end{bmatrix} \begin{bmatrix} v_a \\ T_l \end{bmatrix} \quad (20)$$

$$\begin{bmatrix} i_a \\ w_r \end{bmatrix} = \begin{bmatrix} 1 & 0 \\ 0 & 1 \end{bmatrix} \begin{bmatrix} i_a \\ w_r \end{bmatrix} + [0] \begin{bmatrix} v_a \\ T_l \end{bmatrix} \quad (21)$$

III. CONTROLLERS

A. PI Controller

PI controllers are a combination of a Proportional controller and an Integral controller. The figure below shows a PI controller. The output of the PI controller is proportional to the summation of proportional and integral of the error signal e(t).

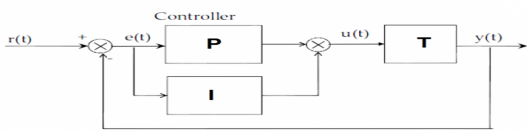


Figure 12 – PI Controller Block Diagram

From the proportionality we get: $u(t) \propto e(t)_p + e(t)_i dt$
Removing the proportional sign and adding the K_p and K_i constants we get: $U(t) = K_p e(t) + \int_0^t K_i e(t) dt$

Where, K_i and K_p proportional constant and integral constant respectively.

B. Cascade Control Technique

Cascade control is a useful prompt rejection of any disturbance to the system before it affects other parts of the system. Basic cascade control system consists of inner and outer control loops. Block diagram below represents simple cascade control.

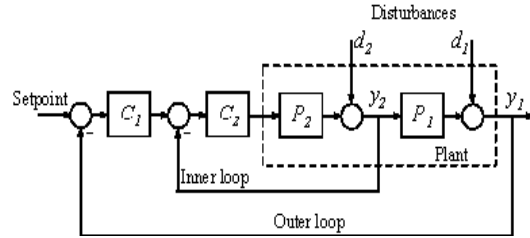


Figure 13 – Cascade Feedback Configuration [12]

C_2 and C_1 are inner and outer loop controllers. P_2 and P_1 are the inner and outer plants. Disturbances are denoted by d_2 and d_1 . Controller C_1 in the outer loop is the primary controller that regulates the primary controlled variable y_1 by setting the reference point of the inner loop. Controller C_2 in the inner loop is the secondary controller that rejects disturbance d_2 locally before it propagates to P_1 . For a cascade control system to function properly, the inner loop must respond much faster than the outer loop.

In our case, both controllers $C_w(s)$ and $C_i(s)$ are PI controllers. Disturbances are in the form of back emf, $E_a(w)$ and load torque T_l . Current controller C_i must respond to change in rotor speed, w , promptly before it affects the stability of the system as a whole. The best practice is to design the inner loop controller C_2 first and then design the outer loop controller C_1 with the inner loop closed. This strategy has been followed while designing the controller.

C. Design of Controller

We started our analysis using Routh-Hurwitz stability criteria to determine the gains of the controllers so that the system is stable at steady state conditions. This method provided us with a large range for the gains of the controllers. This lead to complexity in determining the controller parameters since it required repeated trial and error operation in order to find a set of gain parameter values that would make the system stable. Since Routh-Hurwitz criteria did not prove to be much effective in our case, we shifted our attention towards root locus method. Due to the fact that our system has a closed loop transfer function containing 3rd order of 's' term, analytical solution of the gains is quite complex and tedious using root locus method. The zero-pole cancellation method is thereby used to determine the gains of the controllers easily and in a straightforward manner since it converts the transfer function of the system to 2nd order. Figure 14 depicts a cascade control diagram of the DC motor.

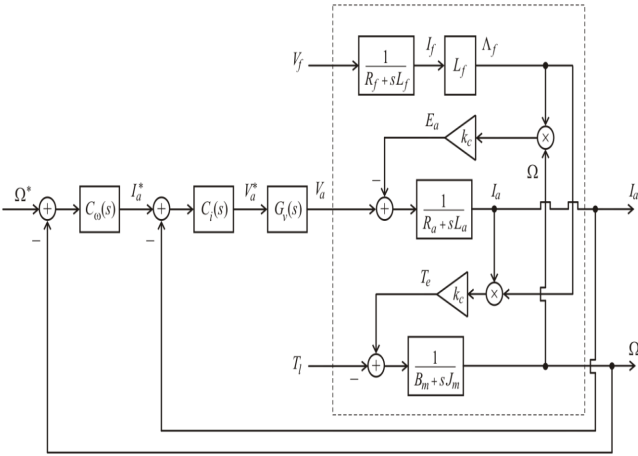


Figure 14 - DC Motor Cascade Control Block Diagram [13]

Assuming that the mechanical variables are constant from the electrical variable perspective, the internal control loop can be simplified as in figure 15.

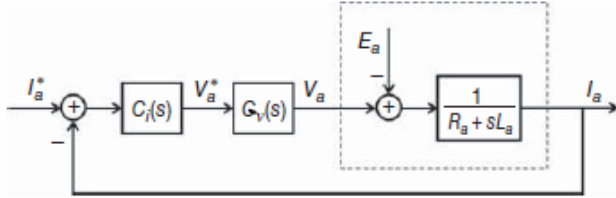


Figure 15 – Internal Control Scheme [13]

The open loop transfer function is given by,

$$F_i(s) = \frac{K_i}{s} \left(s \frac{K_p}{k_i} + 1 \right) \left(\frac{1}{T_v s + 1} \right) \left(\frac{\frac{1}{R_a}}{\frac{L_a}{R_a} s + 1} \right) \quad (22)$$

Cancelling the zero of the controller with the pole of the motor, it yields:

$$F_i(s) = \frac{K_i}{s} \left(\frac{\frac{1}{R_a}}{T_v s + 1} \right) \quad (23)$$

It also provides the inner loop gain ratio as follows:

$$\frac{K_p}{K_i} = \frac{L_a}{R_a} \quad (24)$$

Consequently, the closed loop transfer function of the current controller is given by,

$$M_i(s) = \left(\frac{\frac{K_i}{R_a}}{T_v s^2 + s + \frac{K_i}{R_a}} \right) \quad (25)$$

The gain K_i was obtained making the poles identical.

$$K_i = \frac{R_a}{4T_v} \quad (26)$$

Then the closed loop transfer function becomes:

$$M_i(s) = \frac{1}{(2T_v s + 1)^2} \quad (27)$$

Since T_v is a small value, $M_i(s)$ becomes

$$M_i(s) = \frac{1}{4T_v s + 1} \quad (28)$$

The outer loop of the block diagram shown in figure 14 is given below:

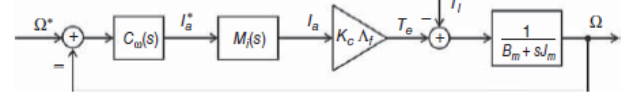


Figure 16 – External loop of the controller [13]

Considering T_l as the disturbance to be compensated by the controller, the open loop transfer function for the speed controller is given by:

$$F_\omega(s) = \frac{\frac{k_i \omega k_c \lambda_f}{B_m} \left(\frac{k_p \omega}{k_i \omega} s + 1 \right)}{s \left(\frac{J_m}{B_m} s + 1 \right) (4T_v s + 1)} \quad (29)$$

Cancelling the zero of the controller with the pole we have

$$F_\omega(s) = \frac{\frac{k_i \omega k_c \lambda_f}{B_m}}{s} \frac{1}{s (4T_v s + 1)} \quad (30)$$

It also provides the outer loop gain ratio as follows:

$$\frac{k_p \omega}{k_i \omega} = \frac{J_m}{B_m} \quad (31)$$

Then the closed loop transfer function is given by:

$$M_\omega(s) = \frac{\left(\frac{k_i \omega k_c \lambda_f}{B_m} \right)}{4T_v s^2 + s + \left(\frac{k_i \omega k_c \lambda_f}{B_m} \right)} \quad (32)$$

The gain $K_i \omega$ was obtained making the poles identical.

$$K_i \omega = \frac{B_m}{16T_v K_c \lambda_f} \quad (33)$$

The closed loop transfer function becomes:

$$M_\omega(s) = \frac{1}{(8T_v s + 1)^2} \quad (34)$$

Equation (24), (26), (31) and (33) were used as design criteria of the controllers. The inner & outer controller gain values were found to be as follows:

$$K_i = 150, K_p = 4.5, k_i \omega = 62.5, k_p \omega = 9375.$$

D. Stability Criteria

It is undesirable for a system to produce a very large change in the response for a small change in input, initial conditions or system parameters. And if the response increases indefinitely then the system is said to be unstable. So it is essential for a system to not only have a desired response but also a stable response. The stability of a system can be split into 2 concepts

- **Bounded Input Bounded Output (BIBO):** As the name suggests if a bounded input is applied to a system, then the output should be bounded.
- **No Input:** If an initial condition is applied, then the system should return to its equilibrium condition on its own.

For a linear time invariant (LTI) system both the concepts are equivalent. There are three popular methods for determining the stability of a system. They are Routh-Hurwitz Stability Criterion, Root Locus Analysis and Nyquist Stability Criterion. In this report the former two are discussed.

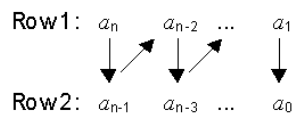
- I) Routh-Hurwitz criterion is a mathematical test that is a necessary and sufficient condition for the stability of a linear time invariant (LTI) control system [1]. It determines the stability of the system using a simple algorithm that provides a range for the controller values (k_p, k_i, k_d) for which the system is stable. The algorithm follows the two-step procedure for a polynomial equation shown below.

a) Polynomial:

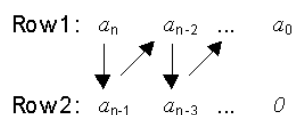
$$a_n s^n + a_{n-1} s^{n-1} + \dots + a_1 s + a_0 = 0$$

- b) Build the Routh array, for rows 1 and 2, build h columns, where $h = \text{Largest integer } [(n+1)/2]$

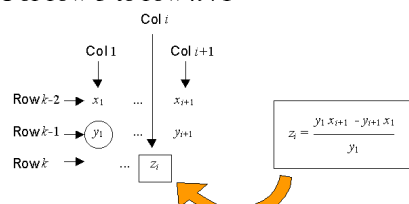
If n is odd:



If n is even:



- c) For row 3 to row $n+1$



- d) Extract the first column of the array and count the number of sign changes. The number of sign changes gives the number of roots of the polynomial which have positive real parts.

In our project, we used the algorithm above to determine the stability of the system and find the range of values of k_p and k_i for our PI controller. Even though it was helpful to do so, it was still not precise enough for optimizing the behavior of the system. That is because we had to assume a value for k_p (within its stability range) only to find a range of values for k_i , which would still guarantee a stable system but not the fastest and most accurate response. To find the most optimized response, we had to use the Root Locus criterion discussed in the next section.

- 2) Root Locus Analysis: The nature of the transient response of a system is determined by the location of poles of its closed loop transfer function. Usually the loop gain (K) is adjustable and the value of the gain locate the poles. So the locus of how these poles by changing the loop gain, is called the root locus plot of the system. Typically for a second order system (eg: $s^2 + as + K = 0$) the root locus is shown in the figure below.

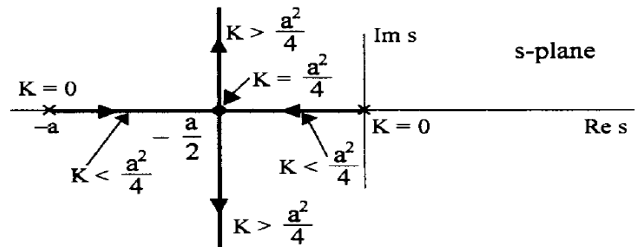


Figure 17 – Root Locus Analysis in S plane [14]

Quite often, the adjustment of the system gain enables the control designer to place the pole at the desired location and if that is not possible then a controller added to manipulate the closed loop poles.

IV. SIMULATION

A. SIMULINK

The schematic of dc motor with controller, as implemented in Simulink is given in figure 18. In Simulink, the simulation was done in s-domain using the gain values of the controllers obtained in analytical approach. The input to the system is step reference speed (ω^*) and the output is the actual speed obtained (ω).

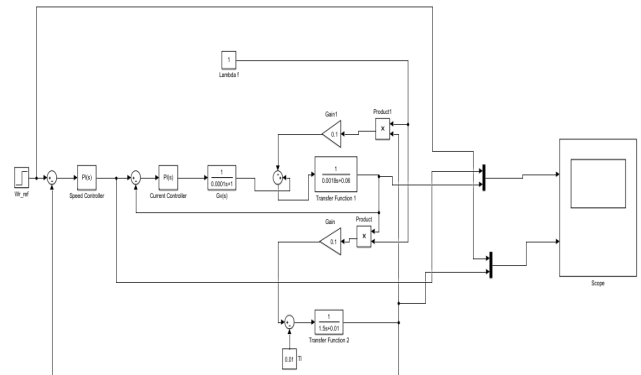


Figure 18 – Schematic of Simulink Diagram

B. MATLAB:

The MATLAB code for the PI controller is obtained using the s-domain analysis by transforming the dynamic equations to t-domain. State space equations were formed as represented in equation (20)-(21). However, it is necessary to discretize the controller itself. Euler integration method was used to discretize this in Matlab simulation. The block diagram model of the PI controller is shown in below figure. From this figure the state space

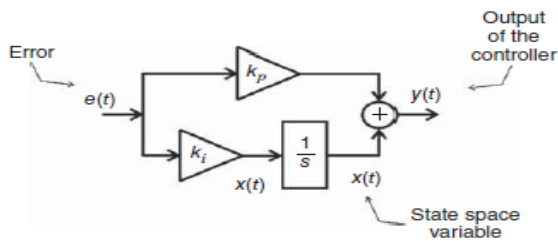


Figure 19 – Block diagram representation of a PI controller [13]

equations for the controller were obtained as follows:

$$\dot{x} = k_i e \quad (35)$$

$$y = x + k_p e \quad (36)$$

For current controller output is Terminal voltage v_a and input is error in armature current ($I_a^* - I_a$). For the speed controller, input and output are $(\omega^* - \omega)$ and I_a respectively.

C. MATLAB Code:

```

close all
clear all
clc

% constants
ra=0.06;
Laa=0.0018;
kf=0.1;
Bm=0.01;
Jm=1.5;
lambdaaf=1;

% initial values of state variables
x1=0;
x2=0;
wr=0;
ia=0;
Va=0;

% input variables
Tl=.01;
Tv=0.0001;

% step size
h=1e-6;
j=0;
t=0;
tmax=0.15;

% speed controller gains
kp1 = 9375; ki1 = 62.5;

% current controller gains
kp2 = 4.5; ki2 = 150;

while t<=tmax
    % simulation time
    if t<0.05
        wr_ref = 10;
    elseif t>0.05 && t<=0.1
        wr_ref = 5;
    else
        wr_ref = -5;
    end

    % Euler's Method
    x2=x2+ki1*(wr_ref-wr)*h;
    ia_ref=x2+kp1*(wr_ref-wr);
    x1=x1+ki2*(ia_ref-ia)*h;
    Va_ref=x1+kp2*(ia_ref-ia);
    Va=Va+((Va_ref-Va)*h/Tv);

    % state space variable 1
    ia = ia + (Va/Laa-ra*ia/Laa-
    kf*lambdaaf*wr/Laa)*h;

    % state space variable 2
    wr = wr + (kf*lambdaaf*ia/Jm-Tl/Jm-
    Bm*wr/Jm)*h;

    % storage the variables
    j = j + 1;
    time(j)=t;
    armature_current(j)=ia;
    armature_ref_current(j)=ia_ref;
    rotor_speed(j)=wr;
    rotor_ref_speed(j)=wr_ref;
    t = t + h;
end

% plotting outputs
figure(1),
subplot(2,1,1),
plot(time,armature_current,time,armature_
_ref_current)
legend('Ia','Ia-ref')
xlabel('Time')
ylabel('Armature Current')
grid minor;
subplot(2,1,2),
plot(time,rotor_speed,time,rotor_ref_spe
ed)
legend('Wr','Wr-ref')
xlabel('Time')
ylabel('Rotor Speed')
grid minor;

```

V. RESULTS AND DISCUSSION

A. Normal Condition

We obtained following armature current and motor speed waveforms as a response to a step reference speed input ($\omega^* = 10$). The output waveforms obtained from Matlab and Simulink are identical. Simulation results indicate that the proposed cascade controller demonstrates excellent performance both in transient and steady state condition. It

also shows null error at steady state condition and faster response time.

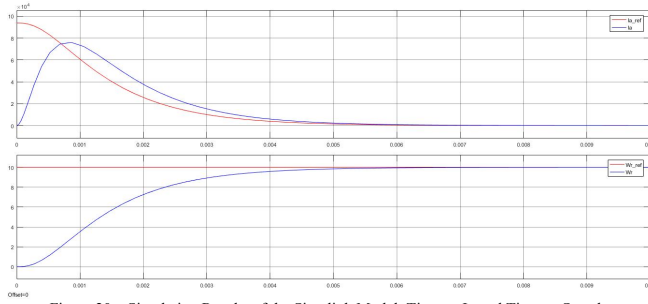


Figure 20 – Simulation Results of the Simulink Model: Time vs I_a and Time vs Speed ω_r

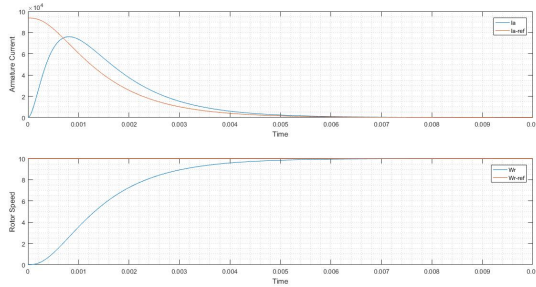


Figure 21 – Simulation Results of the Matlab Code: Time vs I_a and Time vs Speed ω_r

B. Step Change Condition

To check the stability of the system, the reference speed was changed from 10 to 5 and then to -5. The Matlab and Simulink results indicated high stability of the systems since both the current and speed followed the new reference values almost instantly.

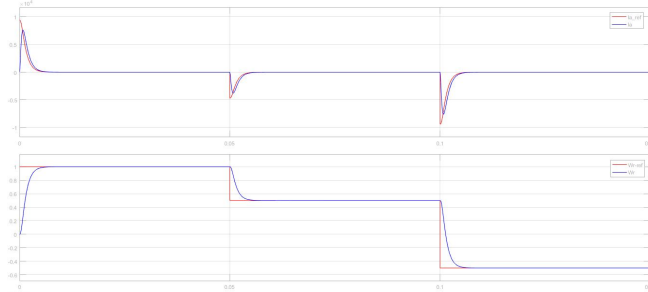


Figure 22 – Simulation Results of the Simulink Model: Time vs I_a and Time vs Speed ω_r at step change condition

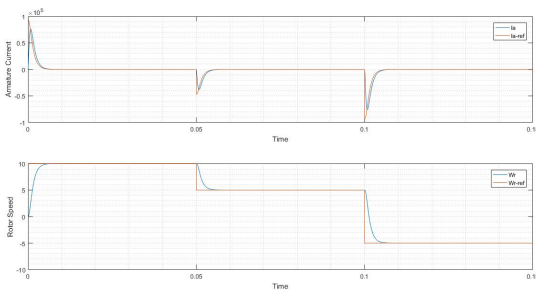


Figure 23 – Simulation Results of the Matlab Model: Time vs I_a and Time vs Speed ω_r at step change condition

C. Faster Pole Cancellation Condition

In our controller design, the dominant pole (ie: slower pole) was cancelled with the zero of the controller to obtain faster response. The faster pole was cancelled this time and the system was simulated to check the response time of the controller. It was observed that the inner loop response time increase a little, whereas the outer loop response time increase drastically.

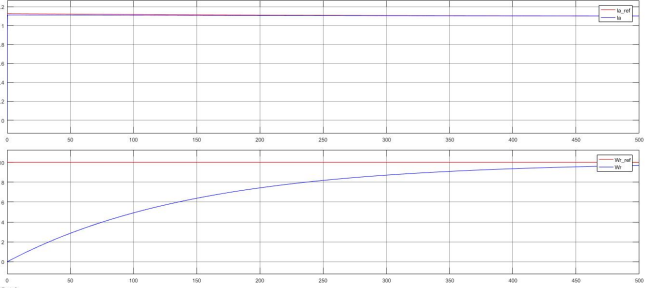


Figure 24 – Simulation Results of the Simulink Model: Time vs I_a and Time vs Speed ω_r when faster pole is cancelled

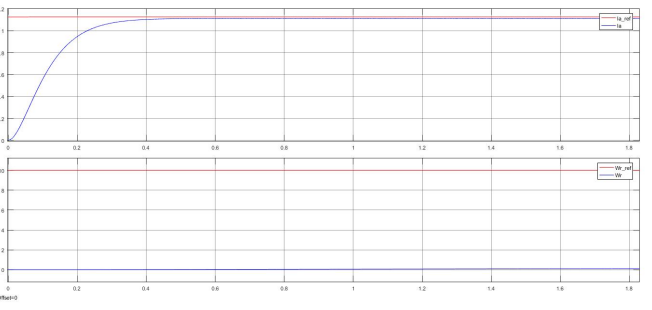


Figure 25 – Simulation Results of the Simulink Model: Time vs I_a and Time vs Speed ω_r , when faster pole is cancelled (I_a is zoomed in).

VI. CONCLUSION

Overall, we believe our design achieved results that sufficiently met the design requirements for this project. While there is no specific requirement in regards to the rate and accuracy of the obtained system frequency response relative to the reference response, our goal was to achieve a response that is asymptotic to the reference response at a rate within fractions of a second, which was successfully accomplished. Moreover, our approach, while not unique, used well-tested and optimized tuning techniques and control methods. However, it should be noted that even though the approach produced excellent results, it is not necessarily appropriate in practical applications. That is because in practice, some of the parameters given in the project assignments such as the armature inductance are not known. Hence, other more experimental approaches such as the Ziegler-Nichols tuning method are used.

REFERENCES

- [1] G. Eason, B. Noble, and I.N. Sneddon, "On certain integrals of Lipschitz-Hankel type involving products of Bessel functions," Phil. Trans. Roy. Soc. London, vol. A247, pp. 529-551, April 1955.
- [2] J. Clerk Maxwell, A Treatise on Electricity and Magnetism, 3rd ed., vol. 2. Oxford: Clarendon, 1892, pp.68-73.
- [3] Routh, E. J. (1877). A Treatise on the Stability of a Given State of Motion: Particularly Steady Motion. Macmillan.
- [4] Learn Engineering, Online source which explains engineering concepts <https://www.patreon.com/posts/dc-motor-how-it-3723184>
Herman, Stephen. Industrial Motor Control. 6th ed. Delmar, Cengage Learning, 2010. Page 251.

- [5] Ohio Electric Motors. DC Series Motors: High Starting Torque but No Load Operation Ill-Advised. Ohio Electric Motors, 2011. Archived November 8, 2011, at WebCite
- [6] "Universal motor", Construction and working characteristics, Retrieved on 27 April 2015.
- [7] Laughton M.A. and Warne D.F., Editors. Electrical engineer's reference book. 16th ed. Newnes, 2003. Page 19-4.
- [8] William H. Yeadon, Alan W. Yeadon. Handbook of small electric motors. McGraw-Hill Professional, 2001. Page 4-134.
- [9] Mathworks, Support Document <https://www.mathworks.com/help/physmod/elec/ref/dcmotor.html>
- [10] Electrical4u, Open and free electrical engineering study site <http://www.electrical4u.com/working-or-operating-principle-of-dc-motor/>
- [11] OpenStax CNX: Sharing Knowledge and Building Communities <http://archive.cnx.org/contents/1b68cd9c-25e7-411d-8513-a5a71a36e8bb@1/speed-and-torque-control> Accessed: December 8, 2016
- [12] Mathworks, Support Document <https://www.mathworks.com/help/control/ug/designing-cascade-control-system-with-pi-controllers.html> Accessed: December 10, 2016.
- [13] S. J. E. C. dos and E. R. C. da Silva, Advanced power electronics converters: PWM converters processing ACvoltages. Hoboken, NJ: John Wiley & Sons Inc., 2015.
- [14] 'Control Systems', N C Jagan, BS Publications